Originally published in *Proceedings of the Fifth International Workshop on Compressible Turbulent Mixing*, ed. R. Young, J. Glimm & B. Boston.
ISBN 9810229100, World Scientific (1996).

A Multi–scale Turbulence Model for Compressible Mixing Flows

D. Souffland[1], O. Grégoire[1], S. Gauthier[1], and R. Schiestel[2]

[1] CEA/L-V 94195 Villeneuve St Georges CEDEX, France

[2] IRPHE 1 Rue Honnorat 13003 Marseille, France

Abstract. A multi-scale closure model for compressible mixing flows is developed. Transport equations for the turbulent kinetic energies and the energy transfer rates are attached to each domain of the turbulent spectrum. The model accounts for the enthalpy production. A Rayleigh-Taylor configuration, and a shock tube experiment, where mixing is induced by Richtmyer-Meshkov instabilities, have been simulated.

1 Introduction

When a shock wave impinges an interface between two different materials, small perturbations of the interface grow, first linearly, then into complex structures, and, under some circumstances, towards a highly evolving and anisotropic turbulence. Then the characteristic length scales, such as the integral scale, the Taylor and the Kolmogorov scales, undergo very rapid changes. Afterwards, turbulence relaxes to an isotropic state until a new process enhances it again. Several single-scale models have already been built to simulate these flows [1, 2, 3]. Since only one spectral scale is considered, these models do not account for the spectral character of the turbulence. In the situations described above, the production mainly occurs in the large scales, then the energy cascades down to the small scales where dissipation acts. As opposed to single-scale models, multi-scale models contain several time and length-scales, which make them well suited to describe non-equilibrium and unsteady situations. In view of this, a multi-scale turbulent model has been derived by partitioning the turbulent kinetic energy spectrum into two regions (section 2). In this paper, we present the preliminary results obtained with this model on simple experimental devices : a Richtmyer-Meshkov induced turbulence in a shock tube in section 3, and a Rayleigh-Taylor flow in section 4. A shock / turbulence interaction in a wind tunnel [4] has also been studied. It will be reported elsewhere.

2 A Two-Scale Model for Compressible Flows

In this section we focus on the derivation of the evolution equations for turbulent quantities. To this end, the spectra of the fluctuating quantities are split into two regions through the definition of a partition wavenumber K_1. The filtering operation is proceeded in the Fourier space. Then for any quantity ϕ, and under the hypothesis of local homogeneity, the correlations of quantities of different spectral domains, such as ϕ_1 and ϕ_2, are equal to zero, i.e. $\overline{\phi_1\phi_2} = 0$ [5]. Here, we use the Favre averaging and we introduce the quantity $w_i = \sqrt{\rho}u_i$ where ρ is the density and u the velocity. Then we have the property $\overline{\rho u_{1i}u_{2i}} = \overline{w_{1i}w_{2i}} = 0$. As a result, the turbulent kinetic energy $\widetilde{k}$ is the sum of two terms $\widetilde{k} = (\overline{\rho u_{1i}u_{1i}} + \overline{\rho u_{2i}u_{2i}})/2\overline{\rho} = \widetilde{k_1} + \widetilde{k_2}$.

The transport equations for $\widetilde{k_1}$ and $\widetilde{k_2}$ are obtained by statistical treatment. These equations contain extra terms which express the energy exchanges between the different regions of the spectrum. The partition wave number is defined as $K_1 = \widetilde{F} \ / \ \widetilde{k_1}^{3/2}$ [6], where $\widetilde{F}$ is the energy flux from the first zone to the second one. The transport equation for $\widetilde{F}$ is derived from the above definition [6]. In accordance with [5], the main production is located at the large scales, where the dissipation is neglected. The energy cascade is expressed by the transfer term $\widetilde{F}$ and the viscous dissipation by $\widetilde{\epsilon}$. Then the set of equations is

$$\overline{\rho}\frac{D\widetilde{k_1}}{Dt} = -\frac{\partial}{\partial x_j}\overline{\rho k_1' u_j'} - (1-\chi)\overline{u_i'}\frac{\partial \overline{P}}{\partial x_i} - \overline{\rho u_{1i}u_{1j}}\frac{\partial \widetilde{U_i}}{\partial x_j} - \overline{\rho}\widetilde{F} \ ,$$

$$\overline{\rho}\frac{D\widetilde{F}}{Dt} = -\frac{\partial}{\partial x_j}\overline{\rho F' u_j'} - C_{F0}\frac{\widetilde{F}}{\widetilde{k_1}}(1-\chi)\overline{u_i'}\frac{\partial \overline{P}}{\partial x_i} - C_{F1}\frac{\widetilde{F}}{\widetilde{k_1}}\overline{\rho u_{1i}u_{1j}}\frac{\partial \widetilde{U_i}}{\partial x_j} - C_{F2}\frac{\overline{\rho}\widetilde{F}^2}{\widetilde{k_1}} \ ,$$

$$\overline{\rho}\frac{D\widetilde{k_2}}{Dt} = -\frac{\partial}{\partial x_j}\overline{\rho k_2' u_j'} - \chi\overline{u_i'}\frac{\partial \overline{P}}{\partial x_i} - \overline{\rho u_{2i}u_{2j}}\frac{\partial \widetilde{U_i}}{\partial x_j} + \overline{\rho}\widetilde{F} - \overline{\rho}\widetilde{\epsilon} \ ,$$

$$\overline{\rho}\frac{D\widetilde{\epsilon}}{Dt} = -\frac{\partial}{\partial x_j}\overline{\rho\epsilon' u_j'} - C_{\epsilon 0}\frac{\widetilde{\epsilon}}{\widetilde{k_2}}\chi\overline{u_i'}\frac{\partial \overline{P}}{\partial x_i} - C_{\epsilon 1}\frac{\widetilde{\epsilon}}{\widetilde{k_2}}\overline{\rho u_{2i}u_{2j}}\frac{\partial \widetilde{U_i}}{\partial x_j} + C_{\epsilon F}\frac{\overline{\rho}\widetilde{\epsilon}\widetilde{F}}{\widetilde{k_2}} - C_{\epsilon 2}\frac{\overline{\rho}\widetilde{\epsilon}^2}{\widetilde{k_2}} \ .$$

The turbulent correlations are modeled with one-point closures. For the Reynolds stress tensor, we modeled the turbulent viscosity by $C_D\overline{\rho}\widetilde{k}^2/\widetilde{F}$ and we suppose turbulence to be isotropic in the small scales region ($\overline{\rho u_{2i}u_{2j}} = 2/3\overline{\rho}\widetilde{k_2}\delta_{ij}$). In the enthalpy production term, we use the classical closure $\overline{u_i'} = -(C_D/\sigma_\rho)(\widetilde{k}^2/\overline{\rho}\widetilde{F})\ (\partial\overline{\rho}/\partial x_i)$ and χ controls the spectral distribution. The model coefficients are determined from the results of simple experiments. This model has been embedded in a 1D hydrocode.

3 Richtmyer-Meshkov Induced Turbulence

Since our final aim is to study hydrodynamic instabilities in ICF context, we simulate Meshkov's experiment in a helium/air shock tube [1]. To initialize the turbulent mixing

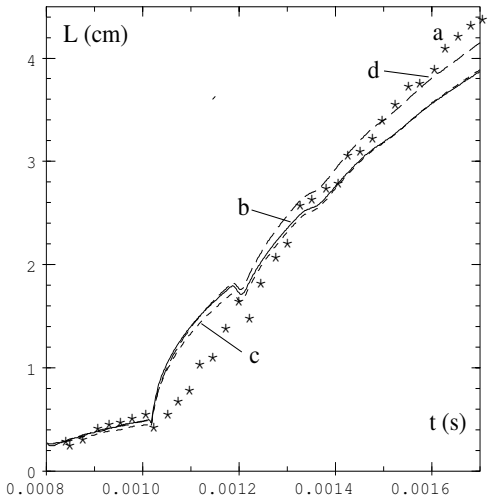

Figure 1: Meshkov's shock tube experiment. Thickening of the TMZ : (a) experimental data of Andronov et al., simulations with (b) the $k-\epsilon$ model and with the two-scale model: (c) $\chi = 0$ and (d) $\chi = 1 - \sqrt{\widetilde{k}_1/\widetilde{k}}$.

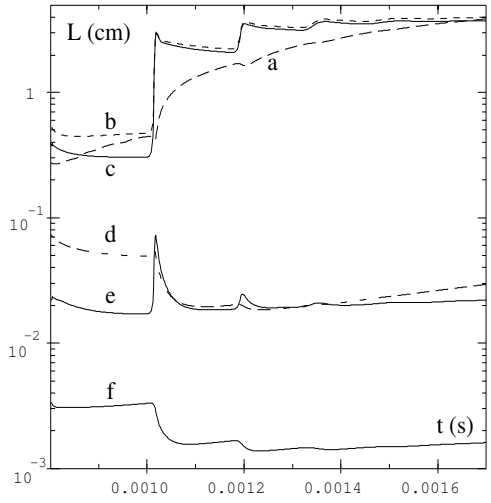

Figure 2: Meshkov's shock tube experiment. Evolution of the characteristic lengths in the two-scale simulation ($\chi = 0$) : (a) TMZ width, (b) integral length $L_\mu = \widetilde{k}^{3/2}/\widetilde{F}$, (c,d) upper bounds of the two spectral regions, (e,f) Taylor and Kolmogorov scales.

zone after the incident shock, we use experimental data for the mixing length and Mikaelian's analysis of the turbulent energy [7].

Fig. 1 displays the experimental data of the turbulent mixing zone (TMZ) thickness, with the results of both single-scale and two-scale models. In these experiments, the turbulent energy is mainly provided by the enthalpic production term during the travelling of shock waves through the mixing zone. The coefficient σ_ρ is calibrated to the value 0.85 against the experiment. Two simulations were carried out with the two-scale model: one with $\chi = 0$; the other with $\chi = 1 - \sqrt{\widetilde{k}_1/\widetilde{k}}$. Numerical results are close to each other. However the distribution of enthalpic production in the two spectral regions ($\chi \neq 0$) seems to increase the mixing length. The comparison on the mixing length does not allow us to decide between the models.

The length scales available with the two-scale turbulence model, where $\chi = 0$, are displayed in Fig. 2.

Fig. 3 shows the evolution of energy fluxes. An interesting feature is the differences in the behaviour of the dissipation terms. After the first reshocks, $\widetilde{\epsilon}$ is lower in the two-scale model than in the classical $k-\epsilon$ model. Moreover, an important delay (40 μs when $\chi = 0$, 70 μs when $\chi \neq 0$) exists between the maxima of $\widetilde{F}$ and $\widetilde{\epsilon}$ after the

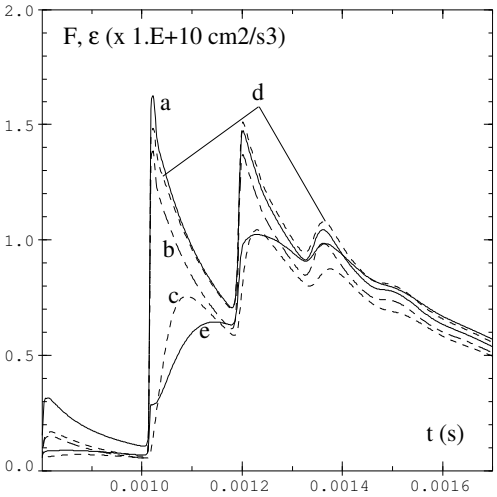

Figure 3: Meshkov's shock tube experiment. Comparison of the energy transfer and the dissipation rates : (a) $\widetilde{\epsilon}$ with the $k-\epsilon$ model, $\widetilde{F}$ and $\widetilde{\epsilon}$ with our two-scale model : (b,c) $\chi = 0$ and (d,e) $\chi = 1 - \sqrt{\widetilde{k_1}/\widetilde{k}}$.

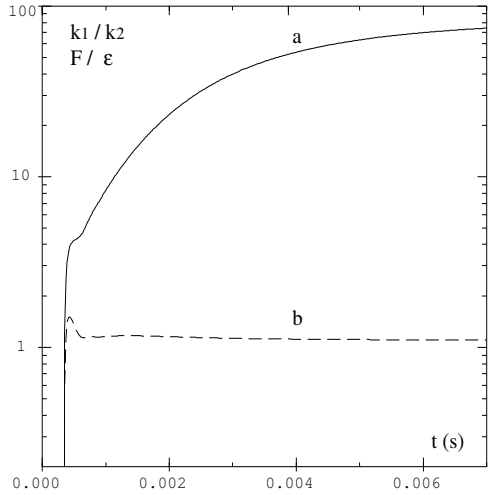

Figure 4: Rayleigh-Taylor configuration. Evolution of (a) the ratio between the turbulent kinetic energies ($\widetilde{k_1}/\widetilde{k_2}$) and (b) the ratio of the energy transfer with respect to the dissipation ($\widetilde{F}/\widetilde{\epsilon}$).

first interaction between the shock wave and the turbulent mixing zone. This delay expresses the expected departure from equilibrium. At the contrary, at the end of the simulation, the three dissipation rates are almost equal, meaning that turbulence has reached an equilibrium state.

4 Rayleigh-Taylor Induced Turbulence

We investigate the turbulent mixing flow at a boundary between two fluids due to Rayleigh-Taylor instability. Similar configurations have been studied experimentally by Read and numerically by Youngs [8, 9], among others. Here, we simulate the mixing of two gases (helium and air) with a constant acceleration $\gamma = 10^7 cm/s^2$. Youngs' relation [9] is used to initialize the turbulent zone. The main interest of this test is that turbulence is continuously fed as opposed to the impulsive production in shock tubes.

The main characteristics of an energy spectrum in which production exceeds dissipation are approximately achieved. Indeed, the proportion of energy in the large scales increases continuously (Fig. 4), and so does the mixing length and the characteristic length of energy containing eddies L_μ. Moreover, as the Kolmogorov length decreases

slowly, the inertial range widens, essentially in the lower part of the spectrum. As we take $\chi = 0$ in these simulations, the small scales region is only supplied with the flux $\widetilde{F}$. The ratio between $\widetilde{F}$ and $\widetilde{\epsilon}$ quickly reaches the asymptotic value 1.1 (Fig. 4), indicating a persistent non-equilibrium turbulent state.

5 Conclusion

This study shows that two-scale models give extra informations with respect to a classical $k - \epsilon$ model, for unsteady configurations where the spectrum is often far away from equilibrium. These models may be supplemented with equations for second order quantities.

References

[1] V.A. Andronov et al., Sov. Phys. Dokl. **44**, 424 (1976) and **27**, 393 (1982).

[2] C.E. Leith, Private communication (1986).

[3] S. Gauthier and M. Bonnet, Phys. Fluids A **2**, 1685 (1990).

[4] D. Alem, Ph. D. Thesis, Université de Poitiers (1995).

[5] R. Schiestel, J. de Mécanique Théor. et Appl. **2**, 417 (1983).

[6] R. Schiestel, *Modélisation et simulation des écoulements turbulents* (Hermès 1993).

[7] K.O. Mikaelian, Physica D **36**, 343 (1989).

[8] K.I. Read, Physica **12D**, 45 (1984).

[9] D.L. Youngs, Physica **12D**, 32 (1984).